


Research Article

Synthesis, Spectral Characterization, and Biological Activities of Some Metal Complexes Bearing an Unsymmetrical Salen-Type Ligand, (Z)-1-(((2-((E)-(2-Hydroxy-6-methoxybenzylidene)amino)phenyl)amino)methylene)naphthalen-2(1H)-one

Quang Trung Nguyen , Phuong Nam Pham Thi, Quang Do Bui, and Van Tuyen Nguyen

Institute of Chemistry, Vietnam Academy of Science and Technology, 18 Hoang Quoc Viet, Cau Giay, Ha Noi, Vietnam

Correspondence should be addressed to Quang Trung Nguyen; trungquang_cnhh@yahoo.com

Received 17 November 2022; Revised 23 December 2022; Accepted 16 January 2023; Published 4 February 2023

Academic Editor: Arun Suneja

Copyright © 2023 Quang Trung Nguyen et al. This is an open access article distributed under the Creative Commons Attribution License, which permits unrestricted use, distribution, and reproduction in any medium, provided the original work is properly cited.

An unsymmetrical salen-type Schiff base ligand, (Z)-1-(((2-((E)-(2-hydroxy-6-methoxybenzylidene)amino)phenyl)amino)methylene)naphthalen-2(1H)-one, and its Zn(II), Cu(II), Co(II), Mn(II), and Fe(III) complexes were synthesized and characterized by mass (MS), nuclear magnetic resonance (NMR), infrared (IR), ultraviolet-visible (UV-Vis) spectra, and effective magnetic moments. The thermal analyses of the obtained ligand and metal complexes were conducted by thermogravimetric analysis (TGA). Antimicrobial activity of the unsymmetrical Schiff base ligand and its metal complexes were examined for *Staphylococcus aureus* as Gram-positive bacteria and *Escherichia coli* as Gram-negative bacteria. *In vitro* anticancer property of synthetic compounds was estimated against human cancer cell lines, a subline of HeLa tumor cell line (KB), and a human liver cancer cell line (HepG-2) as well.

1. Introduction

From the discovery of cisplatin in the mid-1960s, metal-based anticancer candidates have received increasing attention nowadays [1]. Therefore, the development of novel metal-based compounds with potential biological activity has played an important role in bioinorganic chemistry. The nature of the metal and the structure of the organic ligands could be the main factors that can affect the therapeutic activity of such compounds [2].

Salen-type Schiff base ligands with particularly attractive features in their structure and nature are one of the most useful and popular Schiff base ligands [3]. The popularity of tetradentate N₂O₂ bis-Schiff base ligands has come from their possibility of synthesis and ability to coordinate a high diversity of transition metals in various oxidation states and geometries [4, 5]. The bioactivity of metal complexes containing salen-type Schiff base ligands has been considerably

studied. They can show rich biological applications as antibacterial, antifungal, and antitumor activities [6–8]. As usual symmetrical Schiff bases of 1,2- and 1,3-diamines, where the same type of simple aldehydes or ketones are condensed on both nitrogen atoms, and their complexes are extensively reported [9–13]. However, unsymmetrical Schiff bases of diamines where two different carbonyl compounds are conducted on the nitrogen atoms have been paid attention recently [14–16]. Besides the electronic properties of unsymmetrical Schiff bases using different electron donating and/or withdrawing groups at the two imine units [17–19], various ions of transition metals coordinated with these unsymmetrical salen ligands were interestingly needed to study as well. In this research, we continue to report the synthesis and characterization of a new asymmetric salen-type Schiff base (Z)-1-(((2-((E)-(2-hydroxy-6-methoxybenzylidene)amino)phenyl)amino)methylene)naphthalen-2(1H)-one and its Zn(II), Cu(II), Co(II), Mn(II) and Fe(III)

complexes. The antimicrobial activity of a Gram-positive bacterium (*Staphylococcus aureus*) and a Gram-negative bacterium (*Escherichia coli*), as well as *in vitro* cytotoxicity of synthetic compounds against human cancer cell lines, KB and HepG-2, were examined.

2. Materials and Methods

All Chemicals used in this study including *o*-phenylenediamine (98%), 2-hydroxy-1-naphthaldehyde (tech.), Co(OAc)₂·4H₂O, and Mn(OAc)₂·4H₂O have been obtained from Across Organics. The other metal salts such as Zn(OAc)₂·2H₂O, CuCl₂·2H₂O 98.0%, FeCl₃·6H₂O 99.0%, and anhydrous Na₂CO₃ 98.5% were purchased from Xilong Scientific Co., Ltd., China. The solvents were purified by following laboratory procedures. 2-Hydroxy-6-methoxybenzaldehyde was synthesized from 3-methoxyphenol by Reimer-Tiemann reaction [20]: ¹H-NMR (CDCl₃, 500 MHz, δ (ppm), *J* (Hz)): 11.96 (s, 1H-CHO), 10.34 (s, 1H-OH), 7.41 (t, *J* = 8.5, 1H-Ar), 6.52 (d, *J* = 8.5, 1H-Ar), 6.37 (d, *J* = 8.5, 1H-Ar), 3.89 (s, 3H-MeO).

2.1. Instrumentation. A Bruker Advance 500 MHz NMR spectrometer was used to record NMR spectra using d₆-DMSO as the solvent. The high-resolution mass spectrometry (*m/z*) was measured on a Sciex X500 QTOF spectrometer as +IDA-TOF-MS. On Agilent 6310 Ion Trap spectrometer, mass spectra (*m/z*) were determined in electrospray ionization (ESI) mode. FT-IR (KBr pellet, 400–4000 cm⁻¹) spectra were taken with a Perkin Elmer Spectrum Two spectrophotometer. UV-Visible absorption spectra of the synthetic compounds were measured on a Perkin Elmer Lambda UV-35 spectrophotometer in methanol solution (3.0 × 10⁻⁵ M). Magnetic susceptibility measurements of obtained complexes were determined at room temperature using a magnetic susceptibility balance, Mark I with serial No. 25179, of Sherwood Scientific Ltd. Thermogravimetric analysis was carried out on Setaram thermal analyzer, Labsys TG/DSC 1600, under a dynamic flow of air (100 μl/min) and a heating rate of 10°C/min from ambient temperature to about 870°C.

2.2. Synthesis of (Z)-1-(((2-((E)-(2-Hydroxy-6-methoxybenzylidene)amino)phenyl)amino)methylene) Naphthalen-2(1H)-One. This unsymmetrical salen-type ligand was prepared by one-pot method including two-step reaction similarly according to the known procedure [18, 19, 21].

(Z)-1-(((2-((E)-(2-hydroxy-6-methoxybenzylidene)amino)phenyl)amino)methylene)naphthalen-2(1H)-one (**H₂L**): yellow solid, 72.5%; +IDA-TOF-MS (*m/z*) (Figure S1a): 397.1535 [M⁺] (Cal. 397.4459); FT-IR (KBr, cm⁻¹) (Figure S4a): 2924 (ν, C-H), 2615 (ν, O-H), 1607 (ν, C=N), 1562 (ν, C=C), 1470, 1316, and 1250 (ν, C-N), 1185 (ν, C-O), 1089, 824, 738 (δ, C-H), 469; ¹H-NMR (DMSO-*d*₆, 500 MHz, δ (ppm) (Figures S2a and S2b), *J* (Hz)): δ 15.55 (d, *J* = 6.0, 1H, NH), 13.33 (s, 1H, OH), 9.62 (d, *J* = 6.0, 1H, HC=N), 9.12 (s, 1H, HC=N), 8.46 (d, *J* = 8.0, 1H, Naph), 7.91 (t, *J* = 8.0, 2H, Naph), 7.76 (d, *J* = 7.0, 1H, 1H-Naph), 7.50 (t, *J* = 7.0, 1H, Sal),

7.42 (t, *J* = 8.0, 1H, 1H-Ph), 7.42–7.37 (m, 3H, 1H-Naph, 2H-Ph), 7.33 (t, *J* = 7.0, 1H, Ph), 6.96 (d, *J* = 9.0, 1H, Sal), 6.58 (m, 2H, 1H-Naph, 1H-Sal), 3.87 (s, 3H, OCH₃); ¹³C-NMR (DMSO-*d*₆, 125 MHz, δ (ppm)) (Figures S2c and S2d): δ 171.78 (1C, C=O), 161.85 (1C, C=N), 160.39 (1C, C-OH), 160.17 (1C, C-OCH₃), 154.73 (1C, HC-NH), 141.46 (1C, N-C_{Ar}), 137.40 (1C, HN-C_{Ar}), 137.17 (1C, Naph), 135.18 (1C, Naph), 133.16 (1C, Sal), 128.91 (1C, Naph), 128.04 (1C, Naph), 127.68 (1C, Naph), 127.23 (1C, Naph), 126.48 (1C, Ph), 123.43 (1C, Naph), 122.54 (1C, Ph), 120.23 (1C, Ph), 120.08 (1C, Naph), 118.93 (1C, Naph), 109.38 (1C, Ph), 108.73 (1C, Sal), 108.48 (1C, Sal), 101.28 (1C, Sal), 56.01 (1C, OCH₃); UV-Vis (MeOH, 3 × 10⁻⁵ M, λ/nm, ε/cm⁻¹M⁻¹) (Figure S5a): 231 (30,666), 273 (14,667), 336 (14,000), 450 (7,333), 470 (6,667).

2.3. Preparation of Unsymmetrical Salen-Type Complexes. Unsymmetrical salen-type Schiff base complexes of Zn(II), Cu(II), Co(II), Mn(II), and Fe(III) were prepared from the obtained ligand with each metal salt of Zn(OAc)₂·2H₂O, CuCl₂·2H₂O, Co(OAc)₂·4H₂O, Mn(OAc)₂·4H₂O, and FeCl₃·6H₂O in 1 : 1 molecular ratio following the published procedure similarly [22–24] in the presence of Na₂CO₃ and ethanol as solvent.

2.3.1. [Zn(L)·H₂O]. Yellow solid, yield 85%. ESI-MS (*m/z*) (Figure S1b): 458.9 [M-H₂O]⁺ (Cal. 460.8); FT-IR (KBr, cm⁻¹) (Figure S4b): 3207 (ν, O-H, H₂O), 3029 (ν, C-H), 1610 (ν, C=N), 1538 (ν, C=C), 1433, 1380, 1248 (ν, C-N), 1184 (ν, C-O), 1098, 829, 740 (δ, C-H), 551 (Zn-N), 451 (Zn-O); ¹H-NMR (DMSO-*d*₆, 500 MHz, δ (ppm), *J* (Hz)) (Figures S3a and S3b): δ 9.76 (s, 1H, HC=N), 9.40 (s, 1H, HC=N), 8.41 (d, *J* = 7.0, 1H, Naph), 8.09 (dd, *J* = 7.0; 1.0, 1H, Naph), 7.78 (d, *J* = 7.5, 1H, Naph), 7.68 (m, 2H, Naph), 7.46 (dt, *J* = 6.0; 1.0, 1H, Sal), 7.38 (m, 2H, Ph), 7.23–7.18 (m, 2H, Ph), 6.95 (d, *J* = 8.0, 1H, Sal), 6.34 (d, *J* = 7.0, 1H-Sal), 6.07 (d, *J* = 6.5, 1H-Naph), 3.85 (s, 3H, OCH₃); ¹³C-NMR (DMSO-*d*₆, 125 MHz, δ (ppm)) (Figures S3c and S3d): δ 173.72 (1C, C=O), 173.14 (1C, C=N), 161.61 (1C, C-OH), 156.26 (1C, C-OCH₃), 156.03 (1C, HC-N), 140.57 (1C, C_{Ar}-N), 139.60 (1C, C_{Ar}-N), 135.78 (1C, Naph), 135.55 (1C, Naph), 135.07 (1C, Sal), 128.74 (1C, Naph), 127.46 (1C, Naph), 127.14 (1C, Naph), 126.96 (1C, Naph), 126.69 (1C, Ph), 125.61 (1C, Naph), 121.67 (1C, Ph), 119.53 (1C, Ph), 116.93 (1C, Naph), 116.27 (1C, Naph), 115.74 (1C, Ph), 109.73 (1C, Sal), 108.96 (1C, Sal), 94.49 (1C, Sal), 55.72 (1C, OCH₃); UV-Vis (MeOH, 3 × 10⁻⁵ M, λ/nm, ε/cm⁻¹M⁻¹) (Figure S5b): 244 (24,667), 268 (12,000), 335 (13,333), 403 (10,667), 445 (8,000); diamagnetic.

2.3.2. [Cu(L)]. Reddish brown solid, yield 89%. ESI-MS (*m/z*) (Figure S1c): 457.9 [M]⁺ (Cal. 458.9); FT-IR (KBr, cm⁻¹) (Figure S4c): 3064 (ν, C-H), 1602 (ν, C=N), 1532 (ν, C=C), 1433, 1361, 1250 (ν, C-N), 1191 (ν, C-O), 1095, 830, 737 (δ, C-H), 536 (Cu-N), 471 (Cu-O); UV-Vis (MeOH, 3 × 10⁻⁵ M, λ/nm, ε/cm⁻¹M⁻¹) (Figure S5c): 245 (32,667), 270 (22,000), 345 (17,333), 362 (16,667), 425 (13,667); μ_{eff} = 2.03 BM.

2.3.3. [Co(L)]. Brown solid, yield 91%. **ESI-MS** (m/z) (Figure S1d): 453.8 [M]⁺ (Cal. 454.3); **FT-IR** (KBr, cm⁻¹) (Figure S4d): 3033 (ν , C-H), 1603 (ν , C=N), 1527 (ν , C=C), 1455, 1354, 1253 (ν , C-N), 1197 (ν , C-O), 1095, 833, 738 (δ , C-H), 563 (Co-N), 504 (Co-O); **UV-Vis** (MeOH, 3×10^{-5} M, λ/nm , $\epsilon/\text{cm}^{-1}\cdot\text{M}^{-1}$) (Figure S5d): 258 (64,000), 374 (26,333), 470 (13,333); $\mu_{\text{eff}} = 4.34$ BM.

2.3.4. [Mn(L)]. Brown solid, yield 83%. **ESI-MS** (m/z) (Figure S1e): 448.9 [M]⁺ (Cal. 450.3); **FT-IR** (KBr, cm⁻¹) (Figure S4e): 3030 (ν , C-H), 1602 (ν , C=N), 1532 (ν , C=C), 1426, 1366, 1255 (ν , C-N), 1196 (ν , C-O), 1092, 823, 740 (δ , C-H), 557 (Mn-N), 503 (Mn-O); **UV-Vis** (MeOH, 3×10^{-5} M, λ/nm , $\epsilon/\text{cm}^{-1}\cdot\text{M}^{-1}$) (Figure S5e): 247 (43,667), 375 (23,333), 453 (10,333); $\mu_{\text{eff}} = 5.85$ BM.

2.3.5. [Fe(L) (Cl)]. Brown solid, yield 91%. **ESI-MS** (m/z) (Figure S1f): 449.9 [M-Cl]⁺ (Cal. 450.2); **FT-IR** (KBr, cm⁻¹) (Figure S4f): 2924 (ν , C-H), 1597 (ν , C=N), 1533 (ν , C=C), 1456, 1362, 1256 (ν , C-N), 1194 (ν , C-O), 1092, 837, 742 (δ , C-H), 563 (Fe-N), 481 (Fe-O), 411 (Fe-Cl); **UV-Vis** (MeOH, 3×10^{-5} M, λ/nm , $\epsilon/\text{cm}^{-1}\cdot\text{M}^{-1}$) (Figure S5f): 225 (29,000), 272 (15,433), 301 (16,333), 350 (16,667), 433 (8,000); $\mu_{\text{eff}} = 6.08$ BM.

3. Biological Properties

3.1. *Antimicrobial Activity.* *In vitro* antimicrobial activity of **H₂L** and its metal complexes were evaluated using the disk diffusion method [15] against a Gram-positive bacterium, *Staphylococcus aureus* (ATCC 13709), and a Gram-negative bacterium, *Escherichia coli* (ATCC 25922), which were previously grown in Mueller–Hinton Agar (MHA) medium. The tested solutions of 1 mg/mL in DMSO were prepared for all the unsymmetrical salen-type Schiff base ligands and their metal complexes. The MHA (15 mL) kept at ca. 45°C was poured into the 90 mm Petri dishes which were inoculated with the bacterial strains of 100 μL from their culture media (ca. 10^6 CFU/mL) and allowed to solidify. Then, holes of 6 mm diameter were punched carefully. These holes were filled with 50 μL of the tested solutions. Petri dishes were incubated for 24 hrs at 37°C. The diameter of the inhibition zone in millimeters (mm) of each sample was determined and used to evaluate the antimicrobial activity of tested compounds which was performed in Table 1 and Supplementary File S7. Ampicillin was used as the standard reference drug. DMSO alone was used as the negative control under the same condition for each microorganism.

3.2. *Cytotoxicity Assay.* Colorimetric MTT (3-(4,5-dimethylthiazol-2-yl)-2,5-diphenyl tetrazolium bromide) assays were used to estimate *in vitro* cytotoxicity of the unsymmetrical salen-type Schiff base ligand **H₂L** and their complexes against human cancer cell lines, KB and HepG-2, according to Mosmann's modified method [25, 26]. The IC₅₀ (the 50% inhibition concentration was

TABLE 1: Antibacterial activities of the unsymmetrical salen-type ligand and its metal complexes.

Compound	Diameter of inhibition zone (mm)	
	<i>S. aureus</i>	<i>E. coli</i>
H ₂ L	9.0	0
[Zn(L).H ₂ O]	0	0
[Cu(L)]	0	0
[Co(L)]	0	0
[Mn(L)]	16.5	0
[Fe(L)Cl]	12.0	0
Ampicillin	27.0	11.0
DMSO	0	0

defined as the compound concentration causing 50% inhibition of cell growth) values were estimated and presented in Table 2.

4. Results and Discussion

4.1. *Synthesis and Spectral Characterization.* The ligand and complexes were obtained in high yields (72.5 and 83–91%), and they are stable to air and moisture. The synthetic compounds can be dissolved in dichloromethane as well as in methanol, acetonitrile, and dimethylsulfoxide. The ligand was characterized by +IDA-TOF-MS, FT-IR, NMR, and UV-Vis spectra. Its complexes were analysed by ESI-MS, IR, UV-Vis spectroscopies, and magnetic susceptibility. On mass spectra, the pseudomolecular ion signals of the ligand and complexes are found as [M]⁺, [M-H₂O]⁺ or [M-Cl]⁺ which are quite suitable to the calculated masses for suggested formulae.

NMR spectra of the ligand **H₂L** were recorded in DMSO-*d*₆. On ¹H-NMR, there were typical signals of one double peak at 15.55 ppm for 1 NH proton, a single peak at 13.33 ppm for 1 OH proton, a double peak at 9.62 ppm for 1 HC-N proton, and a single peak at 9.12 ppm for HC=N proton. This is proved by tautomerism between enol-imine and keto-amine forms when 1 proton of NH and 1 proton of OH were found (Scheme 1). The protons of aromatic rings were found at 8.46–6.57 ppm and the protons of the CH₃O group at 3.87 ppm as a single peak. On ¹³C-NMR of **H₂L**, there were characteristic signals of C=O carbon at 171.78 ppm, C=N carbon at 161.85 ppm, C-OH carbon at 160.37 ppm, and C-NH carbon at 154.73 ppm. The other aromatic carbon peaks were observed at 141.46–101.28 ppm. The methoxy carbons were found at 56.01 ppm as a single signal. Difference from paramagnetic complexes, the NMR spectra of diamagnetic Zn(II) complex can be recorded by NMR spectrometer. On the ¹H-NMR spectrum, the absence of NH and OH protons for the Zn(II) complex ensured the deprotonation of NH and OH protons upon complexation with Zn(II). The protons of HC-N and HC=N groups at 9.76 and 9.40 ppm, respectively, were shifted downfield compared to the ones of **H₂L** when the coordination was observed. The aromatic protons appeared at 8.41–6.07 ppm, and methoxy protons were found at 3.85 ppm as a single peak reasonably. On the ¹³C-NMR spectrum,

TABLE 2: Cytotoxicity of H_2L and its metal complexes.

Compound	IC ₅₀ (μM)	
	KB	Hep-G2
H_2L	46.14 \pm 3.78	43.29 \pm 3.57
$[\text{Zn}(\text{L})\cdot\text{H}_2\text{O}]$	>250	>250
$[\text{Cu}(\text{L})]$	>250	>250
$[\text{Co}(\text{L})]$	4.45 \pm 0.26	7.40 \pm 0.62
$[\text{Mn}(\text{L})]$	4.68 \pm 0.65	3.67 \pm 0.27
$[\text{Fe}(\text{L})\text{Cl}]$	2.64 \pm 0.11	6.07 \pm 0.44
Ellipticine	1.22 \pm 0.20	1.34 \pm 0.20

the typical signals of C=O at 173.72 ppm, C=N at 173.14 ppm, C-OH at 161.61 ppm, and C-NH at 156.03 ppm were shifted to downfield compared to the free ligand which confirmed the coordination between H_2L with Zn(II) at nitrogen and oxygen atoms. The observed peaks of aromatic carbons were at 140.57–94.49 ppm, and the methoxy carbon was found at 55.72 ppm.

On the IR spectrum of H_2L , the weak broad signal at 2615 cm^{-1} can be attributed to the stretching vibration of the o-O-H group [27]. There are the characteristic signals at 1607 cm^{-1} for the stretching vibration of C=N, at 1250 cm^{-1} for $\nu_{\text{C-N}}$, and at 1185 cm^{-1} for $\nu_{\text{C-O}}$. The disappearance of $\nu_{\text{O-H}}$ and the presence of new bands at 563–536 and 504–451 cm^{-1} for M-N and M-O bondings, respectively, on the IR spectra of the obtained complexes proved the coordination of metals and the ligand [17, 21, 28]. The characteristic bands for $\nu_{\text{C=N}}$, $\nu_{\text{C-N}}$, and $\nu_{\text{C-O}}$ in the complexes are lightly moved to the higher or lower field from the bands in the free ligand. The IR spectra data assured that the coordination of the ligand to the studied metals at nitrogen and oxygen atoms. On the IR spectrum of $[\text{Zn}(\text{L})\cdot\text{H}_2\text{O}]$, there was a typical signal at 3207 cm^{-1} which may be assigned to the stretching vibration of O-H of coordinated H_2O [29–32].

UV-Visible spectra of H_2L and its metal complexes were recorded in methanol solution and presented in Figure 1. The UV-Vis spectrum of H_2L showed main bands at 231–273 nm assigned to the $\pi\text{-}\pi^*$ electronic transition of aromatic rings, at 336 nm relative to $n\text{-}\pi^*$ transition of C=N and C-O groups and at 450 nm attributed to the $n\text{-}\pi^*$ transition within C=O [21, 33]. During the coordination of the ligand to metals, the electronic absorption spectra of synthetic complexes show new MLCT bands at 403 nm for Zn(II) complex, at 425 nm for Cu(II) complex, at 470 nm for Co(II) complex [34–36], at 453 nm for Mn(II) complex, and at 433 nm for Fe(III) complex. The d-d absorptions seem to have no appearance at this complexes' concentration in methanol solution (3×10^{-5} M). The effective magnetic moments were calculated to be diamagnetic for Zn(II) complex [36, 37]. The effective magnetic moments measured experimentally were 2.03 BM corresponding to one unpaired electron supporting the distorted square-planar geometry for Cu(II) complex [37, 38]; 4.34 BM relative to the presence of three unpaired electrons in the octahedral structure for Co(II) complex [33, 37]; 5.85 BM indicated the octahedral geometry for Mn(II) complex [37, 39]; and 6.08 BM due to

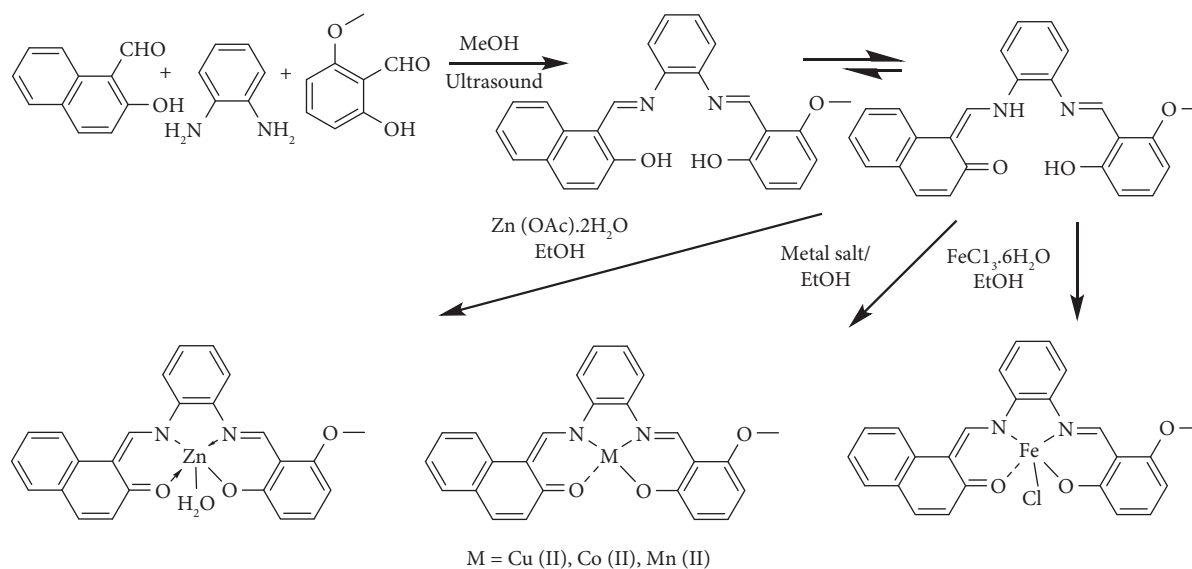
the presence of five unpaired electrons attributed the octahedral structure for Fe(III) complex [37, 40] probably.

4.2. Thermogravimetric Analysis. The thermal analysis of compounds was based on the thermogravimetric analysis (TGA) method at the temperature of 40–870°C. The results of thermal analysis of the ligand and metal complexes in this study based on the degradation steps were used to evaluate the water molecules, the chemical compositions, and the residual amount of the tested compounds (Table 3) (Figures S6a–S6f). The ligand decomposition behaviour comprises two steps in which the first step, decomposition at 140–320°C, is assigned to the loss of methoxy and hydroxy groups (observed about 16.3%, calculated about 16.4%). The second step of thermal decomposition, which occurs at 320–870°C, is assigned to the loss of all most organic compounds (observed at about 76.8%, calculated at 77.5%). Above 870°C, two carbon atoms are still remaining.

The Zn(II), Cu(II), and Mn(II) complexes were decomposed through three steps. The TGA curve of $[\text{Zn}(\text{L})\cdot\text{H}_2\text{O}]$ shows the loss of coordinated water (3.8%) in the range of 150–250°C [32]. Then, the weight reduced by 6.5% can be assigned to the loss of the methoxy group (calc. 6.5%) in the range 250–375°C. The third step of the thermal decomposition, which occurs in the range 375–870°C, could be assigned to the loss of $2\text{C}_4\text{H}_4$ and $\text{C}_{14}\text{H}_7\text{N}_2\text{O}$ groups (67.8%, calc. 67.7%). Finally, the stable compound ZnO is formed above 870°C. The TGAs of other complexes show similar results. The loss of uncoordinated water of $[\text{Cu}(\text{L})]$ occurs at 45–150°C, and then the loss of methoxy and a C_4H_4 group (17.7%, calc. 18.1%) is observed in the range 150–410°C. The loss of remaining C_4H_4 and $\text{C}_{14}\text{H}_7\text{N}_2\text{O}$ groups takes place within the range 410–870°C (57.9, calc. 59.2%), and finally, the stable compound CuO is formed above 870°C [41, 42]. The TGA of $[\text{Co}(\text{L})]$ shows the loss of moisture in the range of 40–150°C. Then, the loss of the methoxy and a C_4H_4 occurs in the range of 150–440°C (18.8%, calc. 18.3%). The weight reduced in the range of 440–850°C (64.4%, calc. 65.1%) can be assigned to the loss of C_4H_4 and $\text{C}_{16}\text{H}_7\text{N}_2\text{O}$ groups. CoO could be found above 850°C [20, 43]. The TGA of $[\text{Mn}(\text{L})]$ performs the loss of uncoordinated water in the range 40–150°C. Then, the loss of methoxy and two C_4H_4 groups occurs in the range of 150–500°C (34.0%, calc. 30.1%). In the range of 500–865°C, the loss of the $\text{C}_{16}\text{H}_7\text{N}_2\text{O}$ group could be recorded (50.0%, calc. 54.1%), and MnO is finally formed above 865°C [24]. The TGA of $[\text{Fe}(\text{L})\text{Cl}]$ showed four decomposition steps. The loss of uncoordinated water takes place within the range of 40–150°C. The loss of HCl gas occurs at 150–375°C (7.7%, calc. 7.5%). Then the loss of methoxy and two C_4H_4 is at 375–630°C, and the loss of the remaining organic group is at 630–870°C. Finally, the stable compound Fe_2O_3 could be obtained above 870°C [44].

4.3. Bioactive Studies

4.3.1. Antimicrobial Activity. In the antibacterial activity study, the unsymmetrical salen-type ligand and its metal complexes were tested against Gram-positive and Gram-negative bacteria, *S. aureus* and *E. coli*, respectively. The



SCHEME 1: Synthesis of the unsymmetrical salen-type ligand and its metal complexes.

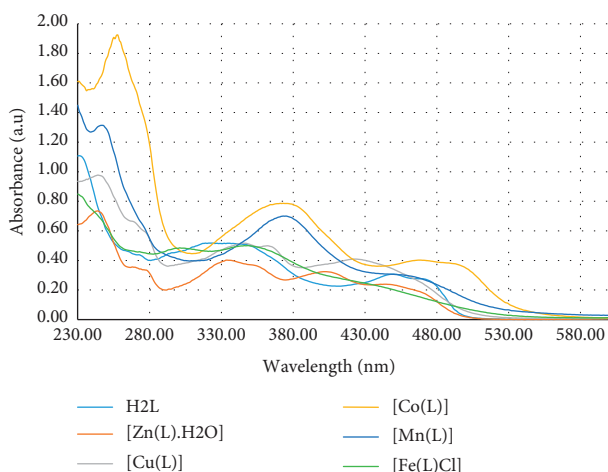


FIGURE 1: Electronic absorption spectra of obtained compounds.

antimicrobial assay was carried out by the disk diffusion method in Muller Hinton–Agar medium using DMSO as the negative control and ampicillin as the positive reference standard. The inhibition efficiencies of the tested compounds shown in Table 1 indicate that the Zn(II), Cu(II), and Co(II) complexes have no activity for both Gram-positive and negative bacteria, *S. aureus* and *E. coli*, respectively. Unsymmetrical Mn(II) and Fe(III) complexes possess the antibacterial potential for only the Gram-positive bacteria, *S. aureus*, better than the ligand **H₂L** with the inhibition zone diameters of 16.5 and 12.0 mm compared with 9.0 mm, respectively. However, their antimicrobial activity is still far from the standard drug, ampicillin, with the inhibition zone diameter of 27.0 mm. The Gram-positive bacteria and Gram-negative bacteria have different cell walls which can induce the different interactions between the tested compounds and bacteria, and some compounds can inhibit only Gram-positive bacteria [37]. Besides the structure and nature of

the ligand, the electronic property of central metals seems to be the main reason which indicates the antibacterial activities of the studied metal complexes, and so some metal complexes are good and effective, but some are infective.

4.3.2. In Vitro Cytotoxicity of H₂L and Its Metal Complexes.

The cytotoxic activity of the metal complexes was tested for human cancer cells, KB and Hep-G2. The obtained results showed that the cytotoxic activity of H₂L is moderate for both human cancer cells with IC₅₀ = 46.14 μM for KB and 43.29 μM for Hep-G2 (Table 2). The complexes [Zn(L)·H₂O] and [Cu(L)] are not active for KB and Hep-G2 (IC₅₀ > 250 μM) when the remaining metal complexes are good active (IC₅₀ < 10 μM) and are more active than the ligand. [Mn(L)] and [Fe(L)Cl] exhibited the best cytotoxicity for Hep-G2 and KB with IC₅₀ = 3.67 and 2.64 μM, respectively.

TABLE 3: TGA data of the ligand and its metal complexes.

Compound	Temperature range (°C)	Weight loss (%)		Assignments
		Found	Calc.	
H ₂ L	150–320	16.3	16.4	Loss of methoxy and hydroxyl groups Loss of all most organic residue 2C atoms
	320–870	76.8	77.5	
	>870	6.9	6.1	
[Zn(L).H ₂ O]	150–250	3.8	3.8	Loss of a coordinated H ₂ O Loss of methoxy group Loss of 2C ₄ H ₄ groups and C ₁₄ H ₇ N ₂ O ZnO and 2C atom
	250–375	6.5	6.5	
	375–870	67.8	67.7	
	>870	21.9	22.0	
[Cu(L)]	45–150	~	~	Loss of uncoordinated H ₂ O Loss of methoxy and C ₄ H ₄ groups Loss of C ₄ H ₄ group and C ₁₄ H ₇ N ₂ O CuO and 2C atom
	150–410	17.7	18.1	
	410–870	57.9	59.2	
	>870	24.4	22.7	
[Co(L)]	40–150	~	~	Loss of uncoordinated H ₂ O Loss of methoxy and C ₄ H ₄ groups Loss of C ₄ H ₄ group and C ₁₆ H ₇ N ₂ O CoO
	150–440	18.8	18.3	
	440–850	64.4	65.1	
	>850	16.8	16.6	
[Mn(L)]	40–150	~	~	Loss of uncoordinated H ₂ O Loss of methoxy and 2C ₄ H ₄ groups Loss of the remain organic C ₁₆ H ₇ N ₂ O MnO
	150–500	34.0	30.1	
	500–865	50.0	54.1	
	>865	16.0	15.8	
[Fe(L)Cl]	40–150	~	~	Loss of uncoordinated H ₂ O loss of HCl gas Loss of methoxy and 2C ₄ H ₄ groups Loss of the remaining organic C ₁₄ H ₇ N ₂ O _{0.5} 1/2 Fe ₂ O ₃ and 2C atom
	150–375	7.7	7.5	
	375–630	29.0	27.7	
	630–870	40.8	43.4	
	>870	22.5	21.4	

5. Conclusion

In this report, (Z)-1-(((2-((E)-(2-hydroxy-6-methoxybenzylidene)amino)phenyl)amino)methylene) naphthalen-2(1H)-one and its Zn(II), Cu(II), Co(II), Mn(II), and Fe(III) complexes were synthesized and characterized by spectrometries. The obtained spectral data supported the tautomerism of the ligand, and it must have one arm in keto-amine and the other in enol-imine form. The synthetic metal complexes have different geometries such as square-planar structure for Cu(II) complex and octahedral geometry for Co(II), Mn(II), and Fe(III) complexes. The thermogravimetric analysis data exhibited uncoordinated and coordinated H₂O in the obtained complexes. The ligand was decomposed almost completely, while metal complexes were decomposed to form the metal oxides. Mn(II) and Fe(III) complexes showed the antibacterial potential for Gram-positive bacteria, *S. aureus*, better than the ligand H₂L. The *in vitro* cytotoxicity for KB and Hep-G2 cancer cell lines indicated that while Zn(II) and Cu(II) complexes have no activity, the metal complexes such as Co(II), Mn(II), and Fe(III) complexes exhibited good cytotoxic activity, much better than the ligand. [Mn(L)] and [Fe(L)Cl] showed the best cytotoxicity for Hep-G2 and KB with IC₅₀ = 3.67 and 2.64 μM, respectively.

Data Availability

All data used to support these research findings are found within the article and in supplementary materials.

Conflicts of Interest

The authors declare that they have no conflicts of interest.

Acknowledgments

The authors express their gratitude to Vietnam NAFOSTED for its financial support in this research by Grant no. 104.01-2018.366.

Supplementary Materials

This section contains the spectral data of the synthetic unsymmetrical tetradentate Schiff base ligand and its Zn(II), Cu(II), Co(II), Mn(II), and Fe(III) complexes (S1–S5). The thermogravimetric analysis (S6) and antibacterial activity (S7) of the synthetic compounds are also included in this file. (*Supplementary Materials*)

References

- [1] N. Muhammad and Z. Guo, “Metal-based anticancer chemotherapeutic agents,” *Current Opinion in Chemical Biology*, vol. 19, pp. 144–153, 2014.
- [2] F. Arnesano, M. I. Nardella, and G. Natile, “Platinum drugs, copper transporters and copper chelators,” *Coordination Chemistry Reviews*, vol. 374, pp. 254–260, 2018.
- [3] D. Ajloo, S. Shabanpanah, B. Shafaatian et al., “Interaction of three new tetradentates Schiff bases containing N2O2 donor atoms with calf thymus DNA,” *International Journal of Biological Macromolecules*, vol. 77, pp. 193–202, 2015.

- [4] M. Karmakar and S. Chattopadhyay, "A comprehensive overview of the orientation of tetradentate N₂O₂ donor Schiff base ligands in octahedral complexes of trivalent 3d metals," *Journal of Molecular Structure*, vol. 1186, pp. 155–186, 2019.
- [5] R. M. Clarke, K. Herasymchuk, and T. Storr, "Electronic structure elucidation in oxidized metal–salen complexes," *Coordination Chemistry Reviews*, vol. 352, pp. 67–82, 2017.
- [6] A. Erxleben, "Transition metal salen complexes in bio-inorganic and medicinal chemistry," *Inorganica Chimica Acta*, vol. 472, pp. 40–57, 2018.
- [7] H. Kargar, A. A. Ardakani, M. N. Tahir, M. Ashfaq, and K. S. Munawar, "Synthesis, spectral characterization, crystal structure and antibacterial activity of nickel(II), copper(II) and zinc(II) complexes containing ONNO donor Schiff base ligands," *Journal of Molecular Structure*, vol. 1233, Article ID 130112, 2021.
- [8] Y. Sun, Y. Lu, M. Bian, Z. Yang, X. Ma, and W. Liu, "Pt(II) and Au(III) complexes containing Schiff-base ligands: a promising source for antitumor treatment," *European Journal of Medicinal Chemistry*, vol. 211, Article ID 113098, 2021.
- [9] P. Seth, M. G. B. Drew, and A. Ghosh, "Functional model for catecholase-like activity: a mechanistic approach with manganese(III) complexes of salen type Schiff base ligands," *Journal of Molecular Catalysis A: Chemical*, vol. 365, pp. 154–161, 2012.
- [10] S. Banerjee, P. Ghorai, P. Sarkar, A. Panja, and A. Saha, "A rare flattened tetrahedral Mn(II) salen type complex: synthesis, crystal structure, biomimetic catalysis and DFT study," *Inorganica Chimica Acta*, vol. 499, Article ID 119176, 2020.
- [11] D. Baecker, O. Sesli, L. Knabl, S. Huber, D. Orth-Holler, and R. Gust, "Investigating the antibacterial activity of salen/salophene metal complexes: induction of ferroptosis as part of the mode of action," *European Journal of Medicinal Chemistry*, vol. 209, Article ID 112907, 2021.
- [12] A. Gusev, V. Shul'gin, E. Braga, E. Zamnius, M. Kryukova, and W. Linert, "Luminescent properties of Zn complexes based on tetradentate N₂O₂-donor pyrazolone schiff bases," *Dyes and Pigments*, vol. 183, Article ID 108626, 2020.
- [13] G. Grivani, S. H. Baghan, M. Vakili et al., "A new copper(II) Schiff base complex containing asymmetrical tetradentate N₂O₂ Schiff base ligand: synthesis, characterization, crystal structure and DFT study," *Journal of Molecular Structure*, vol. 1082, pp. 91–96, 2015.
- [14] N. Mohan, S. S. Sreejith, R. George, P. V. Mohanan, and M. P. Kurup, "Synthesis, crystal structure and ligand based catalytic activity of octahedral salen Schiff base Co(III) compounds," *Journal of Molecular Structure*, vol. 1229, Article ID 129779, 2021.
- [15] H. A. Guadouri, M. Merzougui, D. Hannachi, M. A. Ali, and K. Ouari, "Unsymmetrical salen nickel (II) complex embracing phenol bridge: X-ray structure, redox investigation, computational calculations, antimicrobial and catalytic activities," *Journal of Molecular Structure*, vol. 1242, Article ID 130809, 2021.
- [16] J. Cisterna, V. Artigas, M. Fuentealba et al., "Nickel(II) and copper(II) complexes of new unsymmetrically-substituted tetradentate Schiff base ligands: spectral, structural, electrochemical and computational studies," *Inorganica Chimica Acta*, vol. 462, pp. 266–280, 2017.
- [17] A. A. Nejo, G. A. Kolawole, and A. O. Nejo, "Synthesis, characterization, antibacterial, and thermal studies of unsymmetrical Schiff-base complexes of cobalt(II)," *Journal of Coordination Chemistry*, vol. 63, no. 24, pp. 4398–4410, 2010.
- [18] M. Proetto, W. Liu, A. Hagenbach, U. Abram, and R. Gust, "Synthesis, characterization and in vitro antitumor activity of a series of novel platinum(II) complexes bearing Schiff base ligands," *European Journal of Medicinal Chemistry*, vol. 53, pp. 168–175, 2012.
- [19] Q. T. Nguyen, P. N. Pham Thi, and N. V. Tuyen, "Synthesis, spectral characterization, and in vitro cytotoxicity of some Fe(III) complexes bearing unsymmetrical salen-type ligands derived from 2-hydroxynaphthaldehyde and substituted salicylaldehydes," *Journal of Chemistry*, vol. 2021, Article ID 8028064, 9 pages, 2021.
- [20] Y. B. Vibhute, S. M. Lonkar, M. A. Sayyed, and M. A. Baseer, "Synthesis of substituted 2-hydroxyaryl aldehydes by the microwave-induced Reimer–Tiemann reaction," *Mendeleev Communications*, vol. 17, no. 1, p. 51, 2007.
- [21] D. Çakmak, S. Çakran, S. Yalçinkaya, and C. Demetgül, "Synthesis of salen-type Schiff base metal complexes, electropolymerization on graphite electrode surface and investigation of electrocatalytic effects," *Journal of Electroanalytical Chemistry*, vol. 808, pp. 65–74, 2018.
- [22] G. Ramesh, S. Daravath, M. Swathi, V. Sumalatha, D. Shiva Shankar, and Shivaraj, "Investigation on Co(II), Ni(II), Cu(II) and Zn(II) complexes derived from quadridentate salen-type Schiff base: structural characterization, DNA interactions, antioxidant proficiency and biological evaluation," *Chemical Data Collections*, vol. 28, Article ID 100434, 2020.
- [23] V. A. Shelke, S. M. Jadhav, V. R. Patharkar, S. G. Shankarwar, A. S. Munde, and T. K. Chondhekar, "Synthesis, spectroscopic characterization and thermal studies of some rare earth metal complexes of unsymmetrical tetradentate Schiff base ligand," *Arabian Journal of Chemistry*, vol. 5, no. 4, pp. 501–507, 2012.
- [24] A. S. Alturqi, E. S. Al-Farraj, M. M. Anazy, and R. A. Ammar, "Synthesis, structural identification, DNA interaction and biological studies of divalent metal(II) chelates of 1,2-ethenediamine Schiff base ligand," *Journal of Molecular Structure*, vol. 1219, Article ID 128542, 2020.
- [25] M. V. Berridge, P. M. Herst, and A. S. Tan, "Tetrazolium dyes as tools in cell biology: new insights into their cellular reduction," *Biotechnology Annual Review*, vol. 11, pp. 127–152, 2005.
- [26] K. S. Kumar, V. N. Reena, and K. K. Aravindakshan, "Synthesis, anticancer and larvicidal activities of a novel Schiff base ligand, 3-((2-((1-(4-hydroxyphenyl)ethylidene)amino)ethyl)imino)-N-(p-tolyl) butanamide and its Mn(II), Fe(III), Co(II), Ni(II) and Zn(II) complexes," *Results in Chem*, vol. 3, Article ID 100166, 2021.
- [27] M. Sedighipoor, A. H. Kianfar, G. Mohammadnezhad, H. Görls, and W. Plass, "Unsymmetrical palladium(II) N,N,O,S-Schiff base complexes: efficient catalysts for Suzuki coupling reactions," *Inorganica Chimica Acta*, vol. 476, pp. 20–26, 2018.
- [28] S. Mohebbi and S. Eslami, "Electrocatalytic oxidation of 2-mercaptoethanol using modified glassy carbon electrode by MWCNT in combination with unsymmetrical manganese(II) Schiff base complexes," *Materials Research Bulletin*, vol. 66, pp. 219–225, 2015.
- [29] M. Mohammadikish, "Green synthesis and growth mechanism of new nanomaterial: Zn(salen) nano-complex," *Journal of Crystal Growth*, vol. 431, pp. 39–48, 2015.
- [30] S. S. Sreejith, N. Mohan, N. Aiswarya, and M. P. Kurup, "Inclusion, pseudo-inclusion compounds and coordination polymer of Pd(II), Zn(II) and Cd(II) from salen-type Schiff base ligand with a 1,3-diimino spacer group: crystal

- structures, spectroscopic and thermal studies," *Polyhedron*, vol. 115, pp. 180–192, 2016.
- [31] N. Nuñez-Dallos, A. F. Posada, and J. Hurtado, "Coumarin salen-based zinc complex for solvent-free ring opening polymerization of ϵ -caprolactone," *Tetrahedron Letters*, vol. 58, no. 10, pp. 977–980, 2017.
- [32] A. A. Abdel Aziz, I. H. A. Badr, and I. S. A. El-Sayed, "Synthesis, spectroscopic, photoluminescence properties and biological evaluation of novel Zn(II) and Al(III) complexes of NOON tetradentate Schiff bases," *Spectrochimica Acta Part A: Molecular and Biomolecular Spectroscopy*, vol. 97, pp. 388–396, 2012.
- [33] S. N. Shukla, P. Gaur, M. L. Raidas, and B. Chaurasia, "Tailored synthesis of unsymmetrical tetradentate ONNO schiff base complexes of Fe(III), Co(II) and Ni(II): spectroscopic characterization, DFT optimization, oxygen-binding study, antibacterial and anticorrosion activity," *Journal of Molecular Structure*, vol. 1202, Article ID 127362, 2020.
- [34] S. Celedon, T. Roisnel, D. Carrillo, I. Ledoux-Rak, J. R. Hamon, and C. Manzur, "Transition metal(II) complexes featuring push-pull dianionic Schiff base ligands: synthesis, crystal structure, electrochemical, and NLO studies," *Journal of Coordination Chemistry*, vol. 73, no. 20–22, pp. 3079–3094, 2020.
- [35] I. P. Ejidike and P. A. Ajibade, "Synthesis, characterization, antioxidant, and antibacterial studies of some metal (II) complexes of tetradentate schiff base ligand: (4e)-4-[(2-((E)-[1-(2,4-Dihydroxyphenyl)ethylidene]amino)ethyl)imino]pentan-2-one," *Bioinorganic Chemistry and Applications*, vol. 2015, Article ID 890734, 9 pages, 2015.
- [36] S. Sobha, R. Mahalakshmi, and N. Raman, "Studies on DNA binding behaviour of biologically active transition metal complexes of new tetradentate N2O2 donor Schiff bases: inhibitory activity against bacteria," *Spectrochimica Acta Part A: Molecular and Biomolecular Spectroscopy*, vol. 92, pp. 175–183, 2012.
- [37] A.-N. M. A. Alaghaz, Y. A. Ammar, H. A. Bayoumi, and S. A. Aldhlmani, "Synthesis, spectral characterization, thermal analysis, molecular modeling and antimicrobial activity of new potentially N₂O₂ azo-dye Schiff base complexes," *Journal of Molecular Structure*, vol. 1074, pp. 359–375, 2014.
- [38] S. Meghdadi, M. Amirnasr, M. Majedi et al., "Template synthesis, and X-ray crystal structures of copper(II) and nickel(II) complexes of new unsymmetrical tetradentate Schiff base ligands. Electrochemistry, antibacterial properties and metal ion effect on hydrolysis-recondensation of the ligand," *Inorganica Chimica Acta*, vol. 437, pp. 64–69, 2015.
- [39] L. H. Abdel-Rahman, N. M. Ismail, M. Ismael, A. M. Abu-Dief, and E. A. H. Ahmed, "Synthesis, characterization, DFT calculations and biological studies of Mn(II), Fe(II), Co(II) and Cd(II) complexes based on a tetradentate ONNO donor Schiff base ligand," *Journal of Molecular Structure*, vol. 1134, pp. 851–862, 2017.
- [40] K. S. Kumar and K. K. Aravindakshan, "Synthesis, cytotoxic, anticancer and antimicrobial activities of some metal complexes of a novel tetradentate Schiff base ligand, (E)-3-((2-((E)-1-(2-hydroxyphenyl)ethylidene)amino)ethyl)imino)-N-phenylbutanamide," *Results in Chemistry*, vol. 3, Article ID 100129, 2021.
- [41] P. Deepika, H. M. Vinusha, M. Begum, R. Ramu, P. S. Shirahatti, and M. N. Nagendra Prasad, "2-methoxy-4-(((5-nitropyridin-2-yl)imino)methyl)phenol Schiff base ligand and its Cu(II) and Zn(II) complexes: synthesis, characterization and biological investigations," *Heliyon*, vol. 8, no. 6, Article ID e09648, 2022.
- [42] A. Z. El-Sonbati, M. A. Diab, A. M. Eldesoky, S. M. Morgan, and O. L. Salem, "Polymer complexes. LXXVI. Synthesis, characterization, CT-DNA binding, molecular docking and thermal studies of sulfoxine polymer complexes," *Applied Organometallic Chemistry*, vol. 33, no. 5, Article ID e4839, 2019.
- [43] A. Z. El-Sonbati, M. A. Diab, S. M. Morgan, M. I. Abou-Dobara, and A. A. El-Ghettany, "Synthesis, characterization, theoretical and molecular docking studies of mixed-ligand complexes of Cu(II), Ni(II), Co(II), Mn(II), Cr(III), UO₂(II) and Cd(II)," *Journal of Molecular Structure*, vol. 1200, Article ID 127065, 2020.
- [44] O. Güngör and P. Gürkan, "Potentiometric and antimicrobial studies on the asymmetric Schiff bases and their binuclear Ni(II) and Fe(III) complexes; synthesis and characterization of the complexes," *Arabian Journal of Chemistry*, vol. 12, no. 8, pp. 2244–2256, 2019.